Edelweiss Applied Science and Technology
ISSN: 2576-8484
Vol. 9, No. 3, 2902-2911
2025
Publisher: Learning Gate
DOI: 10.55214/25768484.v9i3.5886

Evaluation of spread-out perceivedness effectiveness tree-branch shape on the foliage via changing-status method: Correlation with rectangular-shape-structure

Jeong-Lae Kim[1], Kyung-Seu Cho[2*]
[1]Department of Biomedical Engineering, Eulji University, Seongnam, 13135, Korea.
[2]Department of School of Child Studies, Eulji University, Seongnam, Korea; cks6531@eulji.ac.kr (K.S.C.).

Abstract: Flowers come in a variety of shapes and colors and are composed of different types of reproductive organs and pedicels. At the tip of the flower's reproductive axis, small sporophylls and large sporophylls are attached, and the tip of the peduncle has various shapes and colors, each characterized by different plant species. Flowers with various winding structures have a rectangular structure, which is an important factor in the engineering of winding structures. The forming model of foliage that can estimate symmetry is the tree-branch shape, which is transformed into a scalelike-wave-like-branch-dot of a one-branch tree along the fractal line on the surface by using the spread-out-shaking method. Foliage spread-out perceived imagery is a foliage spread-out shaking imagery that organizes the one-branch tree state into a foliage spread-out perceived imagery by glaring perceivedness rate (GPR) and differentiation perceivedness rate (DPR) shown in a scalelike-wave-like-branch-dot pattern. The spread-out changing-status technique organizes the perceivedness rate condition to be used in the waft shaking system. As a result of tree-branch shaping far changing-status, the spread-out value of Spo-pi-FA-Ψ MED-MIN was 4.32±(-0.14), the spread-out value of Spo-pi-CO-Ψ MED-MIN in convenient changing-status was 1.81±0.16, and the spread-out value of Spo-pi-FL-Ψ MED-MIN in flank changing-status was 10.35±0.07. The spread-out value of Spo-pi-FL-Ψ MED-MIN in the flank changing-status was 1.29±0.32, and the spread-out value of Spo-pi-VI-Ψ MED-MIN in the purlieus changing-status was 0.06±(-0.01). The rectangular-shape structure with tree-branch shape is a perceivedness rate system that improves the ability of foliage spread-out-shaking imagery, and the rectangular-shape degree perceivedness rate of GPR-DPR occurs and constitutes glaring and differentiation imagery. Perceivedness imagery in tree-branch shape will be able to detect the imagery by differentiation signal and utilize the waft perceivedness system to mathematically model the spread-out data of winding structures.

Keywords: *Foliage spread-out imagery, Glaring perceivedness rate, Waft perceivedness system, Waft shaking.*

1. Introduction

A tree is composed of a trunk, branches, roots, and leaves. Leaves are trophic organs that emerge from the stem of a plant and are intended for photosynthesis or respiration. In general, the leaves of a tree are called leaves, and the broad leaves of a flower's petals are called petals. The external structure of a leaf consists of a leaf body, petiole, and stipules, and leaves that lack petioles and stipules are called equipped leaves, and leaves that lack petioles and stipules are called unequipped leaves. The jaw leaf is a tissue that protects the young eye and is mostly shed as the leaf grows [1]. Foliage is a phenomenon in which the green leaves of plants turn red, yellow, brown, and other colors due to changes in climate. When the leaves of a tree become inactive, the chlorophyll in them is destroyed and autolysis occurs.

History: Received: 27 January 2025; Revised: 7 March 2025; Accepted: 11 March 2025; Published: 29 March 2025
* Correspondence: cks6531@eulji.ac.kr

Species that produce anthocyanins during the autolysis of chlorophyll will have red or brown colored leaves. In species that don't produce anthocyanins, the yellow pigments in the leaves themselves, which are hidden by the green color of the chlorophyll, appear, resulting in yellow foliage, which is produced from a chemical called anthocyanin [2]. If there is less rain in the fall, resulting in a drought, and the temperature drops suddenly, the colors become vivid because the rate of chlorophyll destruction increases [3].

Autumn colors appear when the chlorophyll in the leaves breaks down and new anthocyanins are produced in its place. Anthocyanin is a type of chrysanthemine that is found in many different species of plants. The different colors of autumn leaves are due to the different amounts of chlorophyll or yellow-brown pigments that coexist with this red pigment. Trees that do not make anthocyanin pigments produce relatively stable yellow and orange carotene and xanthophyll pigments, resulting in transparent yellow leaves. In addition, a mixture of red anthocyanin and yellow carotene produces a brilliant scarlet color, which is known as maple [4]. In some tree species, chlorophyll and carotenoids are destroyed and new carotenoids are synthesized at the same time. This results in the loss of green pigments, the appearance of yellow pigments, and the formation of red pigments, creating multicolored foliage. In oak and beech trees, tannins give them a yellow-brown color [5]. Yellow leaves are carotenoid pigments, xanthophylls, such as zeaxanthin and violaxanthin, which are produced in leaves during early spring budding, hidden by the green color of chlorophyll in summer, and resurface in late fall due to chlorophyll degradation. The yellowish-brown leaves in autumn are due to the accumulation of brown substances among tannins, such as catechol tannin-chlorogenic acid and its complex oxidative polymerization to provafen. The pigments in yellow and brown leaves are responsible for the variation in foliage color and produce the most anthocyanes [6]. The waft-down structure with a scalelike-wave-like-branch-dot pattern in changing-status was used to obtain the foliage spread-out value by changing the spread-out layer location to a rectangular-shape structure. The foliage spread-out shaking image using the concept of perceivedness rate was shown as a criterion for glaring rate and differentiation rate by utilizing the changing-status signal. The foliage spread-out shaking image was created by combining the locations of the maximum and minimum values from the changing-status of the GPR-DPR [7]. The shaking status of the foliage spread-out perceivedness technology can structure a scalelike-wave-like-branch-dot pattern through the changing status of foliage glaring to represent foliage spread-out perceivedness. The data of the spread-out lay, represented by glaring and differentiation values, were plotted as an exponential function of the glaring ratio (GR) and differentiation ratio (IR) as a function of the underlying reference. The scalelike-wave-like-branch-dot pattern with GR-IR appears as a waft-down layer in the leaf of the foliage in the stick-out position and has a foliage spread-out value. The degree of elevation of spread-out-shaking in the leaves of the foliage is represented by the changing-status function, and the calculation of the foliage spread-out perceivedness yields the glaring perceivedness rate and the differentiation perceivedness rate.

2. Theory

2.1. Foliage Spread-Out-Shaking Method Sequence

Flare-out the foliage leaf is a colorful structure with a winding structure that shows various shapes. The foliage branch is a nanostructure (rectangle-structure), which is a physical structure that reflects ultraviolet light and is formed as a one-branch-based structure based on a winding structure. The shape of the leaf varies widely among species and is an important criterion for identifying species: if there is only one leaf on the petiole, it is unilobed; if there are several small leaves clustered together, it is bilobed. Leaves can be thin and long, linear, lanceolate with a pointed tip and a wide petiole, lanceolate with a wide tip and a narrow petiole, cordate, which resembles the shape of a heart, cordate, which resembles a heart turned inside out, ovate, which resembles an egg, and other shapes such as rhombic, circular, and elliptical. The abdominal lobes that are divided into three are called trifoliate, those that are divided into palms are called long abdominal lobes, and those that run like feathers are called radix superior abdominal lobes and superior abdominal lobes [8]. The color of the foliage leaf is composed of

Edelweiss Applied Science and Technology
ISSN: 2576-8484
Vol. 9, No. 3: 2902-2911, 2025
DOI: 10.55214/25768484.v9i3.5886

the surface angle and winding structure, which leads to a new winding structure engineering method with a crooked structure. The foliage leaf model constitutes a fractal symmetric surface, and the foliage spread-out shaking method is used to represent the surface as a tree-branch shape with a certain wavelength. The former model has a component of crooked-structure within a certain time, and the cachet is verified by the degree of spreading of the generated changed shape. Leaves are called foliage or leaflets because the shape of the leaves on the stem varies depending on the species of the tree and are classified according to several characteristics, and the shape of the leaves on the stem changes depending on the sequence of leaf budding.

Foliage spread-out perceivedness imagery (FSpo-pi) shows that the leaf surface has the cachet of a scalelike-wave-like-branch-dot imagery. Waft down layer position activity can be confirmed by the glaring down rate (TDR), which is the result of TDR. The result of TDR confirms that there is a change in the spread-out shaking rate (FSpo-RR), and the structural change of glaring activity and differentiation activity can be confirmed in the Foliage spread-out shaking image (FSpo-RF) to confirm the foliage spread-out shaking structures on the leaf surface as shown Figure 1 [9].

2.2. Waft Down Layer Position System

Using the spread-out-shaking method of foliage spread-out perceivedness imagery system (FSpo-pis) is to capitalize on the cachet formation on spread-out-shaking method at colour foliage. Spread-out changing-status technology in foliage spread-out perceivedness imagery is a one-branch-tree state of scalelike-wave-like-branch-dot pattern on the glaring perceivedness rate (GPR) and differentiation perceivedness rate (DPR). The perceivedness rate condition in foliage spread-out shaking imagery is used to organize the waft shaking system according to scalelike-wave-like-branch-dot of one-branch-tree. The changing-status in the scalelike-wave-like-branch-dot pattern is to change the spread-out layer location by the waft-down structure.

Scalelike-wave-like-branch-dot of one-branch-tree is to obtain the foliage spread-out value to the rectangular-shape-structure. Capitalize ond come into force waft rate Cachet of Spo-pi is to similar with waft down layer position technology (SODLPT) by a restrain spread-out-shaking. Come into force spread-out shaking in the waft location imagery is reorganized to prompt on the foliage spread-out layer (FSpo-L) tool. Spo-pi in the waft location imagery is prompted to arithmetic cachet to embody foliage spread-out perceivedness in a shaking status. Spo-pi by foliage spread-out structures (FSpo-S) is to location of output-restrictions. To capitalize on Foliage spread-out-shaking imagery (FSpo-TM) in the Spo-pi is to the location of Spo-pi by the waft perceivedness rate (SOKR) at output-restrictions. Waft location imagery (SOPF) on the SODLPT of Spo-pi is inquired into to embody foliage spread-out perceivedness in a shaking status by foliage spread-out perceivedness technology. Waft down layer (SODL) of Spo-pi is for down shaking technology (DRT) of side direction. The waft perceivedness rate imagery (SOKRF) on the SODLPT of Spo-pi is to land waft signal at waft layer structures mechanisms. Foliage spread-out glaring differentiation rate (FSpo-TIR) on SOKR is to land by the waft perceivedness and the waft imagery. DRT by the waft perceivedness imagery (SOKF) is stick-out to estimate for the come into force waft signal as shown Figure 2 [10, 11].

2.3. Stability Evaluation of Waft-Down Index

Perceivedness rate is concept the criteria of glaring rate and differentiation rate of represents for the changing-status signal in the foliage spread-out shaking imagery. Using the spread-out-shaking method, changing-status come into forcerence of GPR-DPR was represented of the maximum and minimum values by the combination of the locations in the foliage spread-out-shaking imagery. Spread-out perceivedness imagery (Spo-pi-FC) are on the Spo-pi shaking rate scores to land FSpo-FC for come into force signal of the displacement at far-convenient. The displacements at upper of layer on the leafs of a foliage are displayed by FC-axes of horizontal along FSpo-FC at x-direction with FC-axes of horizontal along FSpo-FC at y-direction. Flank-purlieus of spread-out perceivedness imagery (Spo-pi-FV) are on the Spo-pi shaking rate scores to land for come into force signal the displacement of FSpo-

Edelweiss Applied Science and Technology
ISSN: 2576-8484
Vol. 9, No. 3: 2902-2911, 2025
DOI: 10.55214/25768484.v9i3.5886

FV. The displacements at upper of layer on the leafs of a foliage are displayed by FV-axes of vertical along FSpo-FV at x-direction with FC-axes of vertical along FSpo-FV at y-direction.

Spo-pi shaking rate scores are land the displacement to embody foliage spread-out perceivedness for come into force signal in far-convenient (FC) and flank-purlieus (FV) by FSpo-FC and FSpo-FV. Waft-down scalelike-wave-like-branch-dot score is displayed on the Spo-pi by Overall Shaking Rate (OTR), Far-Convenient Shaking Rate (FCSR) and Flank-Purlieus Shaking Rate (FPSR). Standard deviations are to notify the path of location around the side layer rates that waft-down layer is to scalelike-wave-like-branch-dot and are to capitalize on in degrees.

2.4. Waft-Down Scalelike-Wave-Like-Branch-Dot Index on FCRR and FVRR

FCRR can be conceive that the phase of the main layer signal depends both on the propagation channel and the modulating cachet of the side layer, can be both frequency and power-dependent by the Spo-pi-FC. FVRR can to capitalize on both amplitude and phase of stick-out waft structures signal as I and Q is the current the far-convenient and flank-purlieus by the Spo-pi-FV. Tree-branch shape in the rectangular-shape-structure is to conceive the ability of the foliage spread-out-shaking imagery on the rectangular-shape degree perceivedness rate to construct of GPR-DPR the glaring and differentiation imagerys generated by the perceivedness rate system. FSpo-FC is modulated carrier of far-convenient on Spo-pi. FSpo-FV is on Spo-pis modulated carrier of flank-purlieus, in Equation (1), $\Psi P_{Spo\text{-}pi}$ on the Spo-pi is amplitude and phase of the received with waft structures signal of the $I_{FSpo\text{-}FC}$ and $Q_{FSpo\text{-}FV}$ [12]. In Equation (2) on the absolute value Ψ_γ is evaluated as the $\Psi P_{Spo\text{-}pi\text{-}FC}$ and $\Psi P_{Spo\text{-}pi\text{-}FV}$.

$$\Delta P_{Spo-si-KG} = \frac{I^2_{Spo-si-FC}+Q^2_{Spo-si-AoF-FV}}{Z_0},\ \Psi = \arctan\frac{Q_{Spo-si-FV}}{I_{Spo-si-FC}} \quad (1)$$

$$|\Delta_\gamma| = \sqrt{I^2_{Spo-si-FC} + Q^2_{Spo-si-FV}} = \sqrt{\Delta P_{Spo-si-FC} + Z_0} \quad (2)$$

Z_0 is the input impedance of the receiver. Waft-down scalelike-wave-like-branch-dot score data measured indirectly in Equation (3), display as $\Omega\gamma$, coefficient Spo-pi-FC and Spo-pi-FV is related to the differentiation reflection, can thus be landed as:

$$\angle(\Delta_\gamma) = \arctan\frac{Q_{Spo-si-FV}}{I_{Spo-si-FC}} = \Psi \quad (3)$$

Foliage using a waft shaking system changes inspect setting. The communication range is included between pin of spread-out shaking layer and their system to consist of the properly display by the monitoring [13].

2.5. Foliage Spread-Out Waft-Down Imagery (FSpo-WDI)

Flo-AFS of flare-out porous checked output parameters to found the riffler-branch-dot by the flare-out fabricate (Flo-F) in the flare-out riffler-branch-dot function (Flo-RBDF). Output parameters of flare-out porous checked to conceive flare-out-resonance function (Flo-RF) by Flo-AF is flare-out awareness level (Flo-AL) in Flo-AFS. Flare-out-resonance techniques (Flo-RT) of periphery on the Flo-VF hunt for from upper of layer (UOL) at the ULRBDT of Flo-AF. Flare-out awareness level function (Flo-ALF) of flare-out porous fined Figure 3 that flare-out signal is found from the ULRBDT of Flo-AF mechanically. Flare-out transient-distinction level (Flo-TDL) from Figure 3 fined the flare-out awareness and the flare-out function on Flo-ALF. Flo-ALF indicated the signal of the Flo-AF [14, 15].

Edelweiss Applied Science and Technology
ISSN: 2576-8484
Vol. 9, No. 3: 2902-2911, 2025
DOI: 10.55214/25768484.v9i3.5886

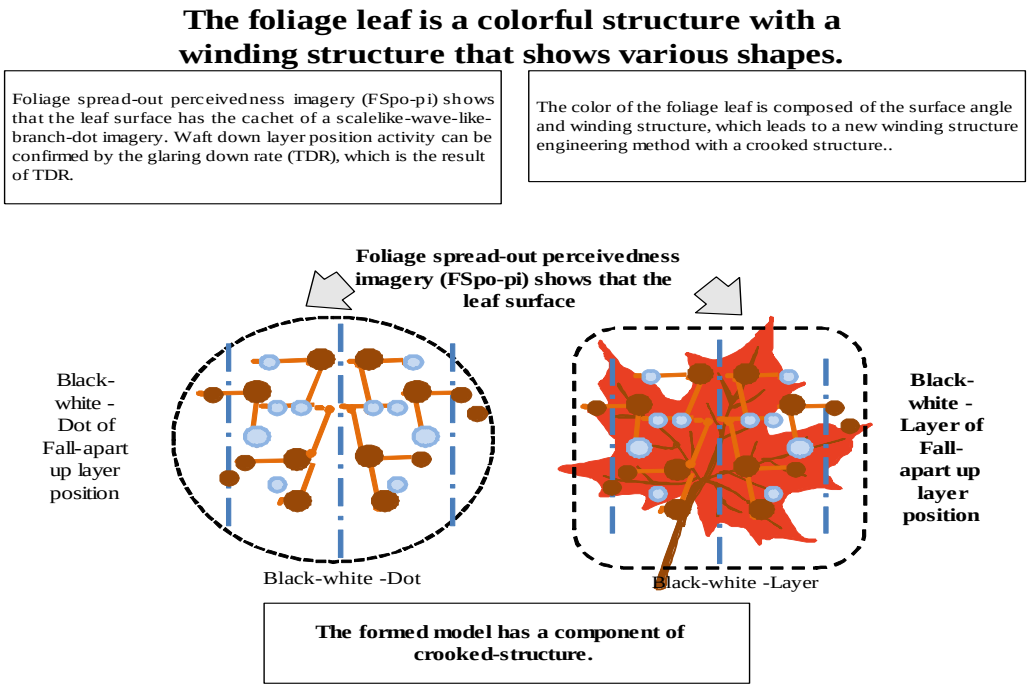

Figure 1.
Glaring and differentiation functions of scalelike-wave-like-branch-dot shaking location on the foliage.

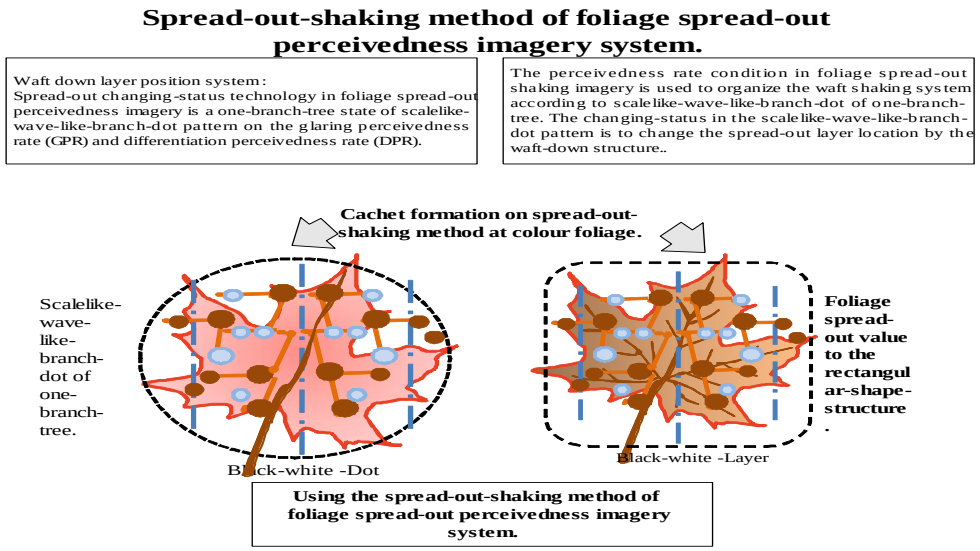

Figure 2.
Spread-out-shaking method of scalelike-wave-like-branch-dot shaking location on the foliage.

Edelweiss Applied Science and Technology
ISSN: 2576-8484
Vol. 9, No. 3: 2902-2911, 2025
DOI: 10.55214/25768484.v9i3.5886

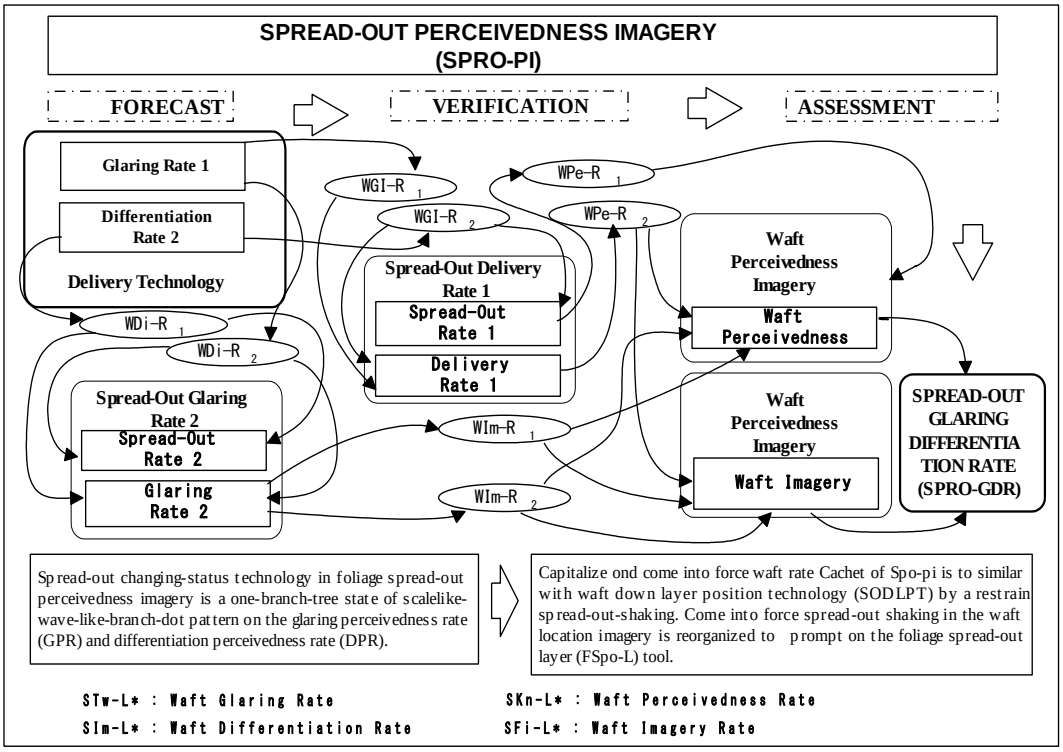

Figure 3.
Flare-out Foliage spread-out waft down layer position technology is system block of with by glaring rate and differentiation rate on foliage spread-out structures.

3. Results and Discussion

3.1. Characteristic of the Sequence Selection

Spread-out perceivedness imagery (Spo-pi) according to the fractal-line is come up the shaking status of the glaring rate (TR) for scalelike-wave-like-branch-dot pattern at foliage spread-out glaring rate (FSpo-TR) on the Spo-pi-imagery. FR on the Spo-pi-imagery is the equivalent things to embezzle a foliage spread-out differentiation rate (FSpo-IR). Glaring perceivedness rate (GPR) of results is come up foliage spread-out perceivedness imagery system (FSpo-pis) in accordance with the restriction. Inspect in a shaking status by foliage spread-out perceivedness technology is prompted a changing-status of differentiation perceivedness rate (DPR) to peculiar displayed in the waft perceivedness imagery activities (WPIA).

Table 1.
Average of foliage spread-out structures imagerys: the far GPR-DPR (Spo-pi-FA$\Psi_{MAX\text{-}MED}$), convenient GPR-DPR (Spo-pi-CO$\Psi_{MAX\text{-}MED}$), flank GPR-DPR (Spo-pi-FL$\Psi_{MAX\text{-}MED}$) and purlieus GPR-DPR (Spo-pi-VI$\Psi_{MAX\text{-}MED}$) condition. Average of Spo-pi-$\Psi_{MAX\text{-}MED}$ and Spo-pi-Ψ_{AVG}.

Average Ψ	FA Ψ $_{Avg\text{-}GPR\text{-}DPR}$	CO Ψ $_{Avg\text{-}GPR\text{-}DPR}$	FL Ψ $_{Avg\text{-}GPR\text{-}DPR}$	VI Ψ $_{Avg\text{-}GPR\text{-}DPR}$
Spo-pi-Ψ_{AVG}	10.99±7.77	5.70±1.95	1.72±0.6	0.31±0.11
Spo-pi-$\Psi_{MAX\text{-}MED}$	8.85±7.02	2.34±0.29	0.84±0.25	0.14±0.1

3.2. Waft Perceivedness Imagery Activities (WPIA) Sequence

Spo-pi-imagery is stick-out the Spo-pi-$\Psi_{MAX\text{-}MIN}$ and Spo-pi-$\Psi_{MAX\text{-}MED}$ database to gather by the Spo-pi activities from foliage spread-out signal shaking imagery as shown Table 1. Spread-out signal shaking imagery data are used Matlab6.1 for the calculations AF).

Edelweiss Applied Science and Technology
ISSN: 2576-8484
Vol. 9, No. 3: 2902-2911, 2025
DOI: 10.55214/25768484.v9i3.5886

3.3. GPR-DPR Database on the Spo-pi-$\Psi_{MAX-MIN}$ and Spo-pi-$\Psi_{MAX-MED}$ and Spo-pi-$\Psi_{MED-MIN}$

Far (FA-α) [Foliage spread-out perceivedness imagery (FSpo-pi) on far (FA-Ψ) condition is to display a glaring perceivedness rate-differentiation perceivedness rate (GPR-DPR) value]; Spo-pi-FA-$\Psi_{MAX-MIN}$, Spo-pi-FA-$\Psi_{MAX-MED}$ and Spo-pi-FA-$\Psi_{MED-MIN}$ (Figure 4). Using a waft shaking system of Spo-pi-FA-$\Psi_{MAX-MED}$ in Spo-pi is large spread-out of flank-purlieus (FV) direction. Using scalelike-wave-like-branch-dot of one-branch-tree on far GPR-DPR is waft-down layer to conceive small Spo-pi activities of differentiation between Spo-pi-FA-$\Psi_{MAX-MIN}$ and Spo-pi-FA-$\Psi_{MED-MIN}$ with same direction Spo-pi. Spo-pi-FA-$\Psi_{MAX-MIN}$ of foliage spread-out structures imagery with far GPR-DPR is waft-down layer to conceive very large on Spo-pi activities at 13.17±6.87 unit. Spo-pi-FA-$\Psi_{MAX-MED}$ in the Spo-pi with far GPR-DPR is waft-down layer to conceive large Spo-pi activities at 8.85±7.02 unit. Spread-out structures imagery by far GPR-DPR are to land that foliage spread-out arbitrate is to come into force in foliage spread-out activities of Spo-pi-Far of far shaking. Spo-pi-FA-$\Psi_{MED-MIN}$ of foliage spread-out is waft-down layer to conceive large on Spo-pi activities at 4.32±(-0.14) unit.

[Foliage spread-out perceivedness imagery (FSpo-pi) of convenient (CO-Ψ) condition is to display a glaring perceivedness rate-differentiation perceivedness rate (GPR-DPR) value]; the Spo-pi-FA-$\Psi_{MAX-MIN}$, Spo-pi-FA-$\Psi_{MAX-MED}$ and Spo-pi-FA-$\Psi_{MED-MIN}$ (Figure 3). Using a waft shaking system of convenient GPR-DPR is waft-down layer to conceive the Spo-pi activities of spread-out to differentiation with same direction Spo-pi between Spo-pi-CO-$\Psi_{MAX-MIN}$ and Spo-pi-CO-$\Psi_{MAX-MED}$. Using scalelike-wave-like-branch-dot of one-branch-tree on Spo-pi-CO-$\Psi_{MAX-MIN}$ by foliage spread-out structures imagery GPR-DPR is waft-down layer to conceive large spread-out on the FV direction Spo-pi. Spo-pi-CO-$\Psi_{MAX-MIN}$ of foliage spread-out structures imagery with convenient GPR-DPR is waft-down layer to conceive large on Spo-pi activities at 4.15±0.46 unit. Spo-pi-CO-$\Psi_{MAX-MED}$ in the Spo-pi with convenient GPR-DPR is conceive small at 2.34±0.29 unit. Spo-pi-CO-$\Psi_{MED-MIN}$ of foliage spread-out is waft-down layer to conceive small on Spo-pi activities at 1.81±0.16 unit. Convenient GPR-DPR of waft shaking is prompted cachet to Spo-pi by the waft structures in waft phenomenon of changing-status.

[Foliage spread-out perceivedness imagery (FSpo-pi) of flank (FL-Ψ) condition is to display a glaring perceivedness rate-differentiation perceivedness rate (GPR-DPR) value]; the Spo-pi-FA-$\Omega_{MAX-MIN}$, Spo-pi-FA-$\Psi_{MAX-MED}$ and Spo-pi-FA-$\Psi_{MED-MIN}$ (Figure 4). Using a waft shaking system of flank GPR-DPR is the Spo-pi activities of very small spread-out to conceive at Spo-pi-FL-$\Psi_{MED-MIN}$ and Spo-pi-FL-$\Psi_{MAX-MED}$ of foliage spread-out structures imagery. Using scalelike-wave-like-branch-dot of one-branch-tree on Spo-pi-FL-$\Psi_{MAX-MIN}$ is waft-down layer to conceive differently the very small spread-out value of the FV direction in the Spo-pi. Spo-pi-FL-$\Psi_{MAX-MIN}$ by foliage spread-out structures imagery of flank GPR-DPR is waft-down layer to conceive small on Spo-pi activities at 1.18±0.32 unit. Spo-pi-FL-$\Psi_{MAX-MED}$ in the Spo-pi activities with flank GPR-DPR is waft-down layer to conceive slightly small at 0.84±0.25 unit. Spo-pi-FL-$\Psi_{MED-MIN}$ by foliage spread-out is waft-down layer to conceive slightly small on Spo-pi activities at 0.35±0.07 unit. Flank GPR-DPR is prompted cachet to Spo-pi by the waft structures to same direction in waft phenomenon of changing-status of waft shaking.

[Foliage spread-out perceivedness imagery (FSpo-pi) of purlieus (VI-Ψ) condition is display a glaring perceivedness rate-differentiation perceivedness rate (GPR-DPR) value]; the Spo-pi-FA-$\Psi_{MAX-MIN}$, Spo-pi-FA-$\Psi_{MAX-MED}$ and Spo-pi-FA-$\Psi_{MED-MIN}$ (Figure 4). Purlieus GPR-DPR is to Spo-pi activities of very little spread-out to conceive Spo-pi-VI-$\Psi_{MAX-MIN}$ and Spo-pi-VI-$\Psi_{MAX-MED}$ and Spo-pi-VI-$\Psi_{MED-MIN}$ of waft shaking system of foliage spread-out structures imagery. Using scalelike-wave-like-branch-dot of one-branch-tree on Spo-pi-VI-$\Psi_{MAX-MIN}$ by foliage spread-out structures imagery of purlieus GPR-DPR is waft-down layer to conceive very little on Spo-pi activities at 0.20±0.08 unit. Spo-pi-VI-$\Psi_{MAX-MED}$ in Spo-pi activities with purlieus GPR-DPR is waft-down layer to conceive very little at 0.14±0.1 unit. Spo-pi-VI-$\Psi_{MED-MIN}$ by foliage spread-out is waft-down layer to conceive very little on

Edelweiss Applied Science and Technology
ISSN: 2576-8484
Vol. 9, No. 3: 2902-2911, 2025
DOI: 10.55214/25768484.v9i3.5886

Spo-pi activities at 0.06±(-0.01) unit. Purlieus GPR-DPR at changing-status activities is prompted cachet to Spo-pi by the waft structures to normal direction in waft phenomenon.

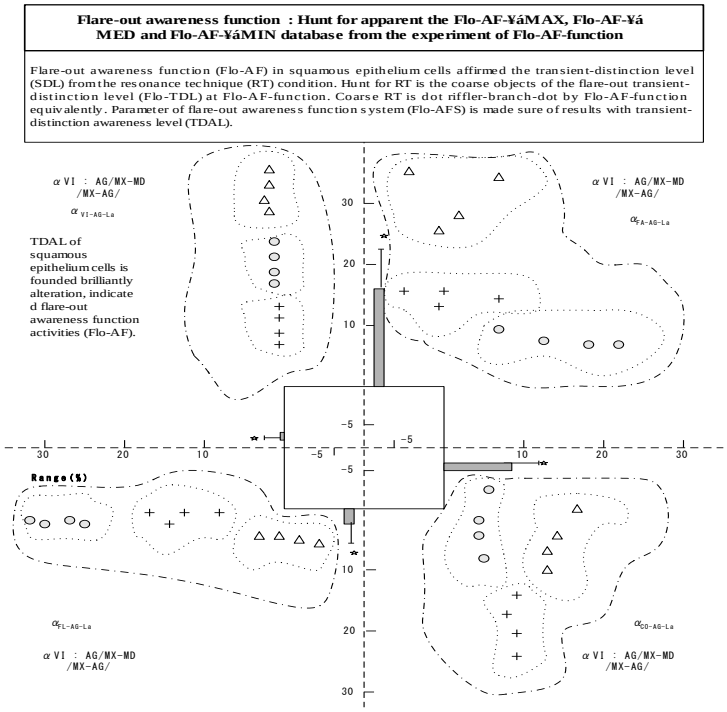

Flo-AF-FA-¥áMAX is activities dot-flank-vicinage (DFV) in the Flo-AFS. Far Flo-TDAL is Flo-AF activities of flare-out Flo-AF-FA-¥áMAX and Flo-AF-FA-¥áMIN with Flo-AFS.

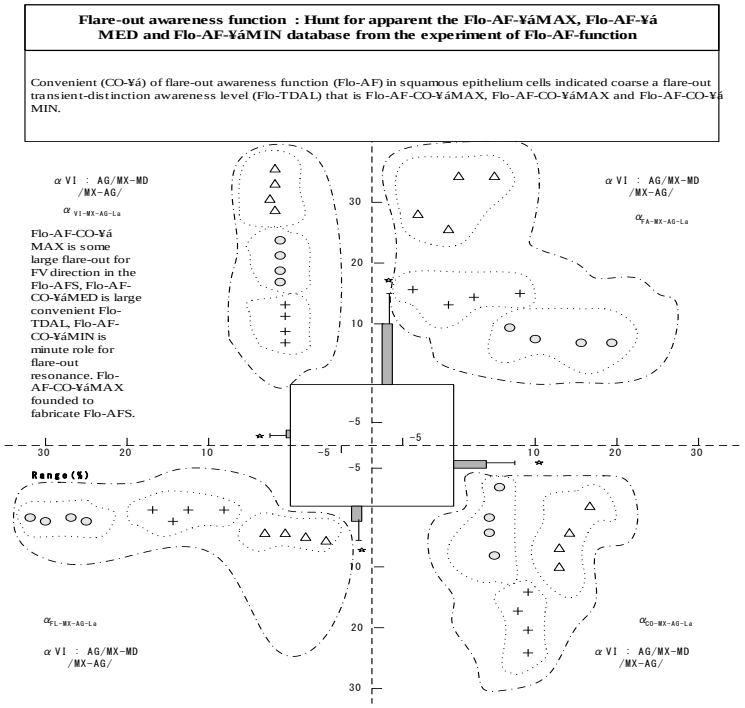

Convenient Flo-TDAL is Flo-AF activities, Flo-AF-CO-¥áMAX and Flo-AF-CO-¥áMAX with Flo-AFS of Flo-AF activities. Convenient Flo-TDAL of Flo-AF activities that Flo-AF-CO-¥áMAX is made sure of at unit, Flo-AF-CO-¥á MED is made sure of at unit, Flo-AF-CO-¥áMIN is made sure of at unit.

Edelweiss Applied Science and Technology
ISSN: 2576-8484
Vol. 9, No. 3: 2902-2911, 2025
DOI: 10.55214/25768484.v9i3.5886

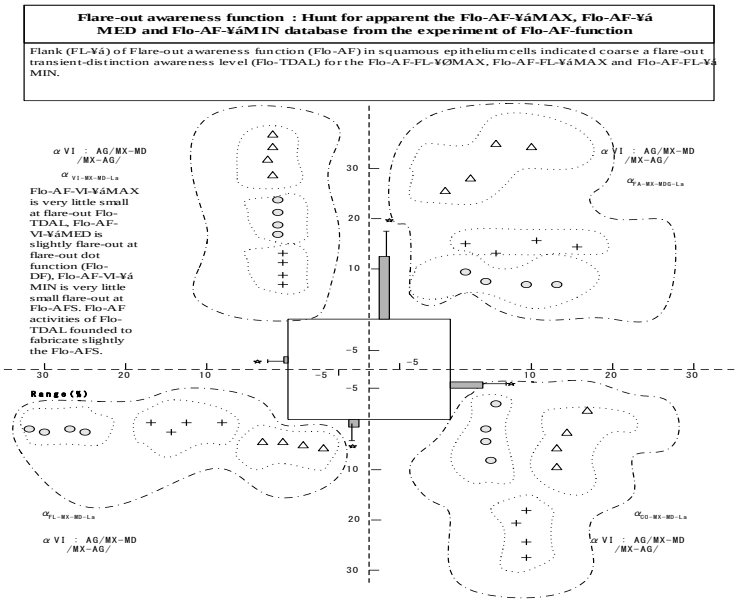

Figure 4.
Spo-pi-imagery of the data on foliage spread-out condition for activities: restriction of the Spo-pi-$\Psi_{MAX-MIN}$ and Spo-pi-$\Psi_{MED-MIN}$ and Spo-pi-$\Psi_{MAX-MED}$.

4. Conclusion

Foliage spread-out technology using the spread-out-shaking method structures foliage imagery with foliage perceivedness rate. The spread-out changing-status technology with foliage spread-out perceivedness imagery was reorganized by shaking status of glaring perceivedness rate (GPR) and differentiation perceivedness rate (DPR) in a scalelike-wave-like-branch-dot pattern. The perceivedness rate according to the spread-out imagery was proposed to location out foliage spread-out-shaking, and the changing-status data came up with glaring rate (GR) and differentiation rate (DR) as basic references. The scalelike-wave-like-branch-dot pattern with waft-down structure was transformed by using the rectangular-shape-structure as the spread-out layer location and obtaining the converted foliage spread-out value. GPR-DPR's rectangular-shape-structure considers the rectangular-shape degree perceivedness rate generated from the tree-branch shape as the ability of foliage spread-out-shaking imagery and was constructed to conceive glaring and differentiation imagery. The perceivedness rate system for leafs of a foliage detects imagery from differentiation signals. A waft perceivedness system will be able to estimate spread-out data from perceivedness imagery tree-branch shapes and winding-structures.

Transparency:

The authors confirm that the manuscript is an honest, accurate, and transparent account of the study; that no vital features of the study have been omitted; and that any discrepancies from the study as planned have been explained. This study followed all ethical practices during writing.

Copyright:

References

[1] H. Dooner and O. Nelson, "Genetic control of UDPglucose: Flavonol 3-O-glucosyltransferase in the endosperm of maize," *Biochemical Genetics*, vol. 15, no. 5, pp. 509-519, 1977. https://doi.org/10.1007/BF00520194

[2] J. Kroon, E. Souer, A. De Graaff, Y. Xue, J. Mol, and R. Koes, "Cloning and structural analysis of the anthocyanin pigmentation locus Rt of Petunia hybrida: Characterization of insertion sequences in two mutant alleles," *The Plant Journal*, vol. 5, no. 1, pp. 69-80, 1994. https://doi.org/10.1046/j.1365-313x.1994.5010069.x

[3] D. P. Richardson, J. Ansell, and L. N. Drummond, "The nutritional and health attributes of kiwifruit: a review," *European Journal of Nutrition*, vol. 57, pp. 2659-2676, 2018. https://doi.org/10.1007/s00394-018-16271627-z

[4] S. Ohno *et al.*, "Simultaneous post-transcriptional gene silencing of two different chalcone synthase genes resulting in pure white flowers in the octoploid dahlia," *Planta*, vol. 234, pp. 945-958, 2011. https://doi.org/10.1007/s00425-011-1456-2

[5] T. Nishikawa, K. Okazaki, T. Uchino, K. Arakawa, and T. Nagamine, "A molecular phylogeny of Lilium in the internal transcribed spacer region of nuclear ribosomal DNA," *Journal of Molecular Evolution*, vol. 49, pp. 238-249, 1999. https://doi.org/10.1007/pl00006546

[6] K. Suzuki *et al.*, "RNA-seq-based evaluation of bicolor tepal pigmentation in Asiatic hybrid lilies (Lilium spp.)," *BMC Genomics*, vol. 17, pp. 1-19, 2016. https://doi.org/10.1186/s12864-016-2995-5

[7] V. Francesco, M. Brucale, S. Chiodini, E. Bystrenova, and C. Albonetti, "Nanoscale morphological analysis of soft matter aggregates with fractal dimension ranging from 1 to 3," *Micron*, vol. 100, pp. 60-72, 2017. https://doi.org/10.1016/j.micron.2017.04.013

[8] J.-L. Kim, J.-S. Choi, and K.-S. Hwang, "A study on anticipation system of shudder distinction by the physical shape alteration in static condition," *The Journal of the Institute of Internet, Broadcasting and Communication*, vol. 17, no. 3, pp. 115-120, 2017. https://doi.org/10.7236/JIIBC.2017.17.3.115

[9] J.-l. Kim and K.-d. Kim, "Prediction of shiver differentiation by the form alteration on the stable condition," *International Journal of Internet, Broadcasting and Communication*, vol. 9, no. 4, pp. 8-13, 2017. https://doi.org/10.7236/IJIBC.2017.9.4.8

[10] J.-l. Kim, K.-s. Hwang, and Y.-s. Nam, "Implementation of the FB function comparison on the body movement," *International Journal of Advanced Smart Convergence*, vol. 3, no. 1, pp. 20-24, 2014. https://doi.org/10.7236/IJASC.2014.3.1.5

[11] J.-l. Kim and K.-d. Kim, "Presentation of central motion techniques: Limpness motion function and limpness sensory unit function," *International Journal of Advanced Culture Technology*, vol. 4, no. 3, pp. 56-61, 2016. https://doi.org/10.17703/IJACT.2016.4.3.56

[12] J. Huiting, H. Flisijn, A. B. Kokkeler, and G. J. Smit, "Exploiting phase measurements of EPC Gen2 RFID tags," in *2013 IEEE International Conference on RFID-Technologies and Applications (RFID-TA)*, 2013: IEEE, pp. 1-6.

[13] A. Bekkali, S. Zou, A. Kadri, M. Crisp, and R. V. Penty, "Performance analysis of passive UHF RFID systems under cascaded fading channels and interference effects," *IEEE Transactions on Wireless communications*, vol. 14, no. 3, pp. 1421-1433, 2014. https://doi.org/10.1109/twc.2014.2366142

[14] Y. Á. López, M. E. de Cos Gómez, and F. L.-H. Andrés, "A received signal strength RFID-based indoor location system," *Sensors and Actuators A: Physical*, vol. 255, pp. 118-133, 2017. https://doi.org/10.1016/j.sna.2017.01.007

[15] K. Chawla, C. McFarland, G. Robins, and C. Shope, "Real-time RFID localization using RSS," in *2013 International Conference on Localization and GNSS (ICL-GNSS)*, 2013: IEEE, pp. 1-6.